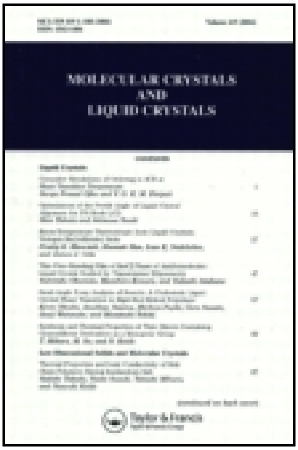

Molecular Crystals and Liquid Crystals Science and Technology. Section A. Molecular Crystals and Liquid Crystals

Holographic Recording, Using Liquid Crystalline Side Chain Polymers

Klaus Anderle [a] & Joachim H. Wendorff [a]

[a] Deutsches Kunststoff-Institut Darmstadt, D-6100 Darmstadt, Germany and Fachbereich Physikalische Chemie, Philipps-Universität, Marburg, 3550, Marburg

Version of record first published: 24 Sep 2006.

To cite this article: Klaus Anderle & Joachim H. Wendorff (1994): Holographic Recording, Using Liquid Crystalline Side Chain Polymers, Molecular Crystals and Liquid Crystals Science and Technology. Section A. Molecular Crystals and Liquid Crystals, 243:1, 51-75

To link to this article: http://dx.doi.org/10.1080/10587259408037761

Mol. Cryst. Liq. Cryst., 1994, Vol. 243, pp. 51–75
Reprints available directly from the publisher
Photocopying permitted by license only

Printed in the United States of America

Holographic Recording, Using Liquid Crystalline Side Chain Polymers

KLAUS ANDERLE and JOACHIM H. WENDORFF

Deutsches Kunststoff-Institut Darmstadt, D-6100 Darmstadt, Germany and Fachbereich Physikalische Chemie, Philipps-Universität Marburg, 3550 Marburg

The review describes the principles of a holographic storage process based on the liquid crystalline state of organic polymeric materials. Such materials are capable of forming anisotropic glasses, which can be obtained as thin films. By suitable means one is able to align the optical axis of the uniaxial system within the film along a given direction or parallel to the film normal. A storage process is made possible by incorporating into the polymer a suitable dye—such as azobenzene—characterized by the fact that it is able to undergo a light-induced isomerization process even in the solid glassy state. This in turn leads to a reorientation of the optical axis within the film and thus to strong modifications of the optical properties. The information written-in in this way can be erased either by heating to temperatures above the glass transition temperature or by light. The paper describes the physical processes involved in the storage process and the capability of such materials to store holograms. Of particular interest is that the novel type of storage material is not only able to store information on amplitude and phase (scalar properties) of the light but also on the state of polarization. It may thus be used for polarization holography.

Keywords: liquid crystalline polymers, holographic storage, polarization holography

I. INTRODUCTION

In the past decade optical recording and the development of suitable recording media have become a subject of extensive scientific and industrial interest. High optical sensitivity, an enhanced storage density and short switching as well as access times are as important as, in certain applications, reversibility and high signal to noise ratio after many write-erase cycles.

A sizable number of different nonrewritable optical storage media (write once) have been developed employing various techniques. At present the most important technology uses the magneto-optical Kerr rotation in thin magnetic films.[1] A second concept is based on thin metallic layers which are locally switched from the polycrystalline solid state to the amorphous state and vice versa by transient heating.[2] The reflectivity of the illuminated spot is thus reversibly changed. Both approaches introduced so far have advantages and inherent problems. In any case a digital recording technique is employed.

In principle also storage via the recording and the read out of a hologram is feasable.[3,4] Some of the advantages are in this case that the writing and read out can be done in a parallel rather than in a serial fashion which speeds up the optical processing considerably and that the safety of the stored information is strongly enhanced. The requirement is of course to have materials at hand which allow to store and erase a hologram. The concepts introduced above do not allow such kind of technology.

This review is concerned with a different technology based on the liquid crystalline state and on organic polymeric materials.[5-7] This class of materials is capable of forming anisotropic glasses, which can be obtained as thin free standing films or films on substrates. By suitable means to be described below in some detail one is able to align the optical axis of the uniaxial system within the film along a given direction or parallel to the film normal.[8,9] Thus an optically homogeneous uniaxial film is obtained, the optical birefringence being typically of the order of 0.1–0.2. A storage process is made possible by incorporating a suitable dye such as an azobenzene dye in the polymer for which one is able to induce an isomerization process by means of light in the solid glassy state.[9-13] The isomerization process is connected with a change of the geometry of the dye. This in turn leads, as we and subsequently others have demonstrated,[14-20] to a reorientation of the optical axis within the film and thus to strong modifications of the optical properties. The information written in this way can be erased by local or global heating to temperatures above the glass transition temperature. Erasure by light is also possible. In the following we will describe the physical processes involved in the storage process and the capability of such materials to store holograms. We will show that the novel type of storage material is not only able to store information on amplitude and phase (scalar properties) of the light but also the state of polarization. It may thus be used for polarization holography.[15,16]

II. THE CONCEPT OF HOLOGRAPHIC IMAGING

In all conventional parallel recording methods such as photography a flat picture of a three-dimensional object is recorded on a light sensitive film/surface. It is just the intensity distribution of the light scattered by the object at the flat recording

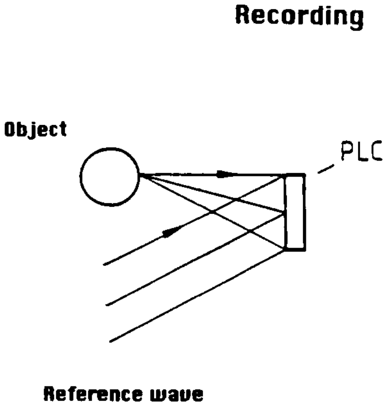

FIGURE 1 Recording of a hologram (schematic).

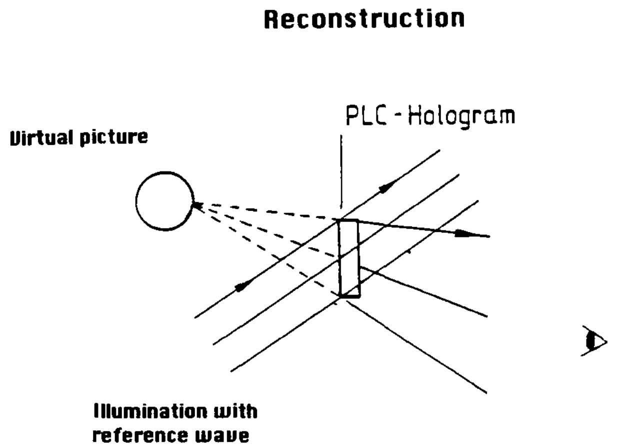

FIGURE 2 Reconstruction of a hologram (schematic).

surface which is stored. Thus all information on the relative phases of the light waves coming from different points of the object, i.e. information about the optical path differences to different parts of the object is lost. The unique feature of holography is the idea of recording the complete wave field: amplitude and phase of the waves scattered by the object. Since all recording media are only sensitive to intensity it is necessary to convert the phase information into variations of intensity.[3,4] This is done by using a coherent illumination, as shown in Figure 1 and by superimposing a planar or spherical reference wave and the wave scattered by the object: an interference pattern due to the two waves is recorded. The intensity at any point in this pattern (hologram) depends on the phase as well as the amplitude of the original wave. Thus the hologram stores information both on the amplitude and phase of the object wave. The original object wave can be reconstructed simply by illuminating the hologram with the reference wave, as shown in Figure 2. The observer sees a three dimensional image of the object which exhibits all the natural effects of perspective and depth of focus characteristic of the real object. An important feature as far as optical information storage is concerned is that one piece of information is not just stored at one particular location in the recording medium where it may be destroyed by a local defect but rather at every single location in the film.

The simplest hologram one can think of is obtained by superimposing two planar waves. This leads to a characteristic periodic intensity modulation in the plane of the recording film and thus to an optical grating in the material. Its characteristic features which can be read out by a planar wave (periodicity of the grating, the amplitude of modulation of the optical properties) allow to obtain valuable information on the storage capability of the recording material (diffraction efficiency, resolution, etc., see below). A second type of a simple hologram is obtained by the superposition of a planar and a spherical wave which gives rise to a Fresnel type interference pattern. The hologram stored in a recording film can be considered as an optical element manufactured by holography (HOE: holographic optical component). It can be used as a Fresnel lens to enlarge the size of an object or to decrease its size.[20]

This contribution will not focus so much on the use of holograms for optical information storage and processing but rather on the characterization of the liquid crystalline polymers usuable for holographic storage and on the particular aspect of their capability to record polarization holograms. Yet some basic facts should be introduced.

Information can in principle be stored quite densely in a microfilm. Yet the maximum storage density is limited in this case among others by dust or scratches which can result in a complete loss of parts of the information. Holographic storage has the advantage that surface damages do not erase any particular piece of information but just leads to an increase of the signal to noise ratio. This makes it possible to use materials with much higher resolution. In addition several holograms may be stored in one and the same recording film. A selective read out is possible by appropriate means. Finally the topic of associated storage should briefly be mentioned. One feature of interest is that in this case the read out of a partial set of information may induce the read out of a whole set of informations well beyond the one apparently asked for: i.e., the holographic storage yields associations. The particular properties of associated storage allow to use holograms for character recognition.[21]

III. MATERIALS USED AND PREPARATION OF THE LCP-BASED RECORDING FILMS

The compounds used are predominantly nematic side chain polymers with acrylate or polyester-type chain backbone. Examples are shown in Figure 3. The polymers contain azobenzene-units in different concentrations. This allows the tailoring of absorption, optical and dielectric properties more or less at will, depending on the choice of copolymer. The synthesis has been the topic of many previous publications.[5–7] To prepare the films used for storage the liquid crystalline polymers were routinely annealed above their glass transition temperature in a vacuum oven to remove residual solvent. Prefabricated LCD-cells of various sizes and thicknesses were filled at temperatures well above the clearing temperature by capillary action. The cells consist usually of two quartz substrates which were covered by spin coating with a thin polyamide layer. This layer was subsequently structured by a buffing technique. Defect free and large size (as large as 25 cm^2) homogeneous monodomain films of high optical quality can be achieved by annealing the cells at temperatures close to but still below the clearing temperature.

UV-dichroitic measurements are used to characterize the alignment of the liquid crystalline side groups both with respect to the principal axis and with respect to the degree of orientational order, in terms of the scalar order parameter S. Figure 4 displays a polar diagram of the extinction measured on a monodomain. The extinction is measured at 360 nm (characteristic for the azobenzene group) as a function of the angle between the plane of the polarization and the rubbing direction which corresponds to the direction of the nematic director. The results show that

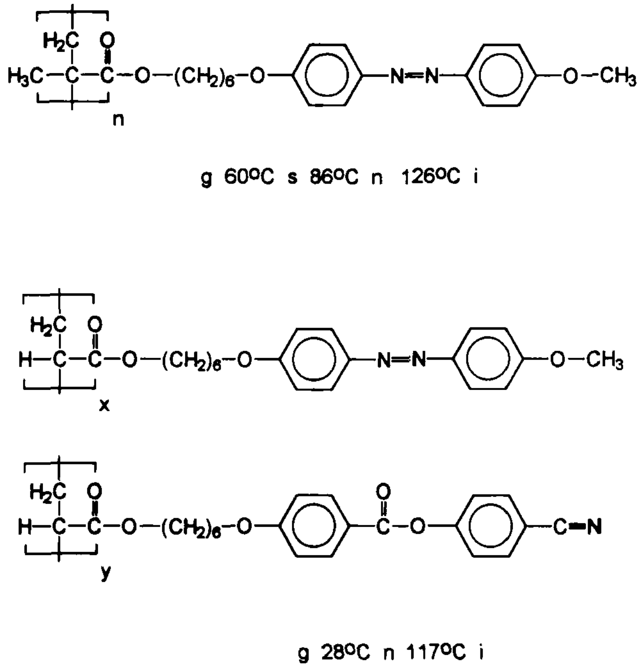

FIGURE 3 Chemical structure of some of the polymers used for optical storage.

the orientation is perfect along the rubbing direction and that the order parameter S obtained from

$$S = \frac{E_p - E_s}{E_p + 2E_s};$$

(where E_p and E_s are the extinctions with polarized light parallel and perpendicular to the director direction (the dipole transition moment is oriented along the symmetry axis of the molecules)) is of the order of 0.6. This value and its temperature dependence are directly reflected in the birefringence Δn

$$\Delta n = \Delta n_0 S;$$

where Δn_0 corresponds to the saturation value for $S = 1$.

This is apparent from Figure 5. The birefringence increases stepwise from zero values within the isotropic melt and with decreasing temperature in the nematic phase. The upper value achieved for Δn is about $\Delta n = 0.25$. This is thus the modulation of the refractive index which can be induced by switching the director, provided one is able to reorient the director homogeneously by up to 90° relative to the polarization of the light.

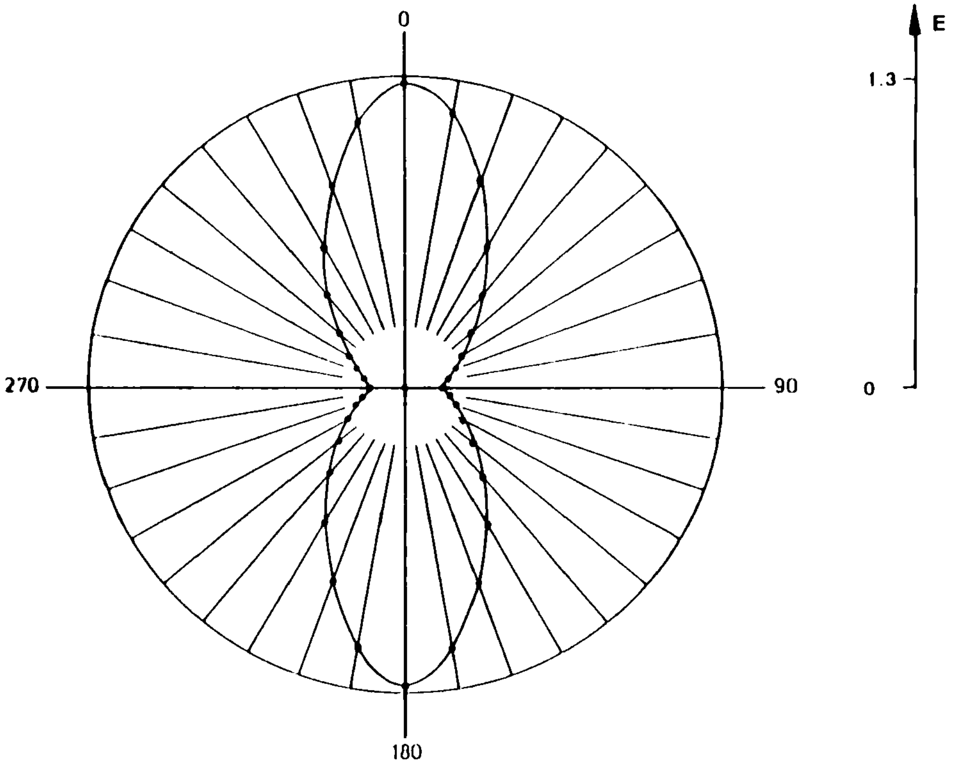

FIGURE 4 Polar diagram of the extinction, as obtained for a nematic monodomain for a side chain liquid crystalline polymer.

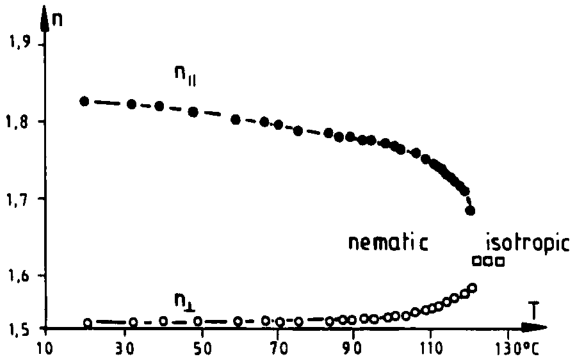

FIGURE 5 Variation of the ordinary and extraordinary index of refraction with temperature for a side chain liquid crystalline polymer in the nematic and isotropic state.

IV. BASIC MECHANISM CONTROLLING THE STORAGE PROCESS: REORIENTATION BY PHOTOSELECTION

In principle the director direction of a nematic monodomain film can be switched by electric fields, as in the case of liquid crystalline display. This holds also for the high frequency electromagnetic field. The disadvantage of such a mechanism for optical storage is apparent at once if one considers the main features of this process. It is characterized by the fact that a threshold value exists for the applied field:

$$U_0 = \pi(K/\varepsilon_0\Delta\varepsilon)^{1/2}$$

which is controlled by the particular curvature elastic properties of liquid crystalline phases (curvature elastic coefficient K) and the anisotropy of the dielectric constant $\Delta\varepsilon$. The consequence in terms of optical storage is that a threshold intensity exists for writing which is typically of the order of several 1–100 kW/cm^2. In addition the response times τ given by the following expressions for rise (active) and decay (passive)

$$\tau_r^{-1} = \tau_d^{-1}((U/U_0)^2 - 1)$$

$$\tau_d^{-1} = (\pi/d)^2K/\gamma$$

are controlled by the rotational viscosities γ. The passive response times are of the order of ms for low molar mass liquid crystals, of the order of *s* to min for polymer side chains and diverge as the glass transition temperature is approached. On the other hand we would like to store information optically in a solid film, i.e., in a film with a viscosity which should ideally be infinite. The solution is to use a storage mechanism which does not depend on the macroscopic viscosity but rather a local one. Such a mechanism is the trans-cis isomerization of azobenzene containing dyes[10,11] which happens without any threshold intensity and which is known to happen in the glassy state, actually even at temperatures of the order of 10 K.

The modulation of the optical properties of monodomains of liquid crystalline polymers is achieved by the trans-cis isomerization which is caused by the interaction of light with the convalently attached azobenzene groups of the polymer. This reversible photoreaction is well characterized for low molar mass compounds and amorphous polymers[12,13] but has been analyzed for liquid crystalline polymers only recently.[14-20, 22-24] This type of reaction is of particular interest in a liquid crystalline state: the cis isomer is bent and nonmesogenic and hence cannot form a liquid crystalline phase. Thus the changes accompanying the photoreaction (rod-like to bend conformation) may result in the loss of the capability to induce a liquid crystalline state. So one effect related to the isomerization is that the liquid crystalline phase is destabilized and eventually destroyed as a consequence of the illumination with light.

Figure 6 shows a polar diagram of the extinction after illumination. It is apparent that the degree of orientational order (order parameter S) has been strongly reduced. This reaction has been proposed as the basis of a storage technology related to thermal recording: the irridation leads to a transition into the isotropic state, the reaction back to the trans state can be induced optically using another wavelength or thermally since the trans state is thermodynamically favorable. Thus the liquid crystalline state can be erased and restored locally, yet the previously defined preferred direction has been erased. This gives rise to scattering spots, i.e. optical

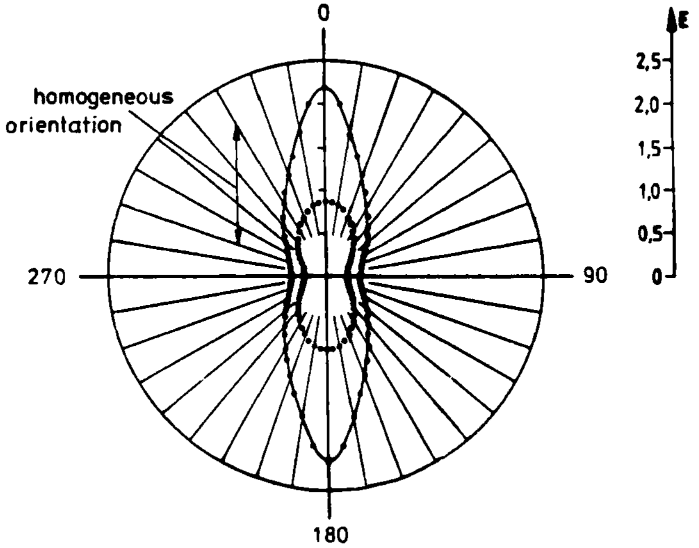

FIGURE 6 Polar diagram of the extinction, as obtained for a nematic monodomain for a side chain liquid crystalline polymer before (-•-) and (••) after irradiation with unpolarized light.

recording is possible. This process happens either due to circularly polarized or depolarized light of sufficient intensity.

A totally different storage process can be induced if linearly polarized light is used and if the illumination is done in such a way that the liquid crystalline state is not destablized. Typically intensities of the order of mW/cm^2 rather than kW/cm^2 are used. In particular the illumination can be performed within the liquid crystalline glassy state, i.e., using solid films. The experimental finding is that by using polarized light one is able to reorient the director significantly. Figure 7 shows the polar diagram of the extinction prior to and after illumination with polarized light. The saturation value of the reorientational angle amounts to 90° with respect to the polarization direction of the light. This result is independent of the relative orientation of the polarization direction with respect to the director, as shown in Figure 8. This modulation of the direction of the nematic director is directly reflected in the variation of the birefringence (Figure 9) as measured within the plane of the film and perpendicular to it using a wave guide technique. The birefringence is reduced and the sign of the birefringence is reversed due to the induced director reorientation.

We have proposed a phenomenological description of this effect which is able to account at least for the principal phenomena found for all liquid crystalline systems.[22] The model is based on the following concept:

1. A chromophore which is subjected to an isomerization cycle changes its direction within the glassy state more or less randomly due to the variation of its geometric shape from a stretched to a bent configuration. Only those groups can change their orientation which undergo such an isomerization cycle.

2. The reorientation is the effect of the local mobility within the glassy state as controlled by free volume fluctuations and of a partial or complete memory loss

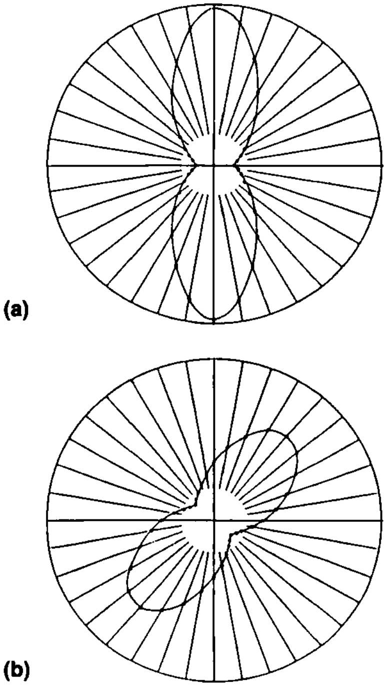

FIGURE 7 Polar diagram of the extinction, as obtained for a nematic monodomain for a side chain liquid crystalline polymer (a) before and (b) after irradiation with polarized light.

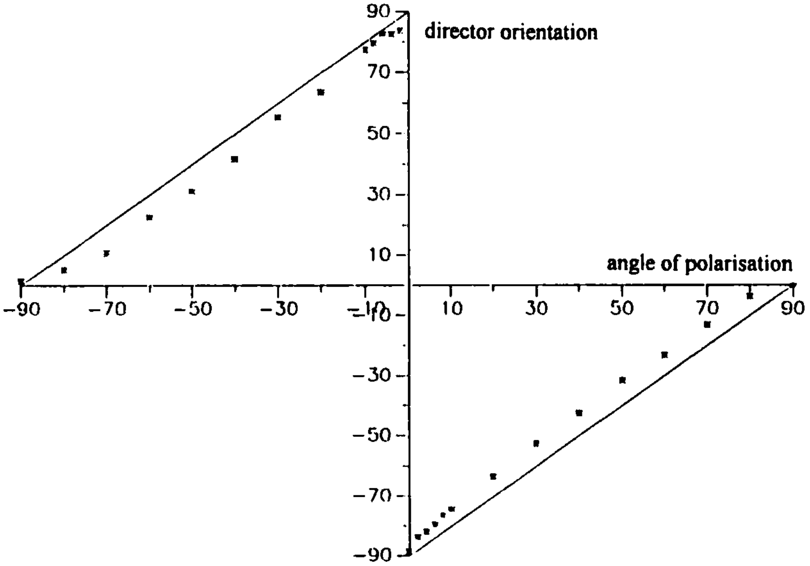

FIGURE 8 Dependence of the orientation of the director after irradiation with polarized light on the original relative orientations of the polarization of the light and the nematic director.

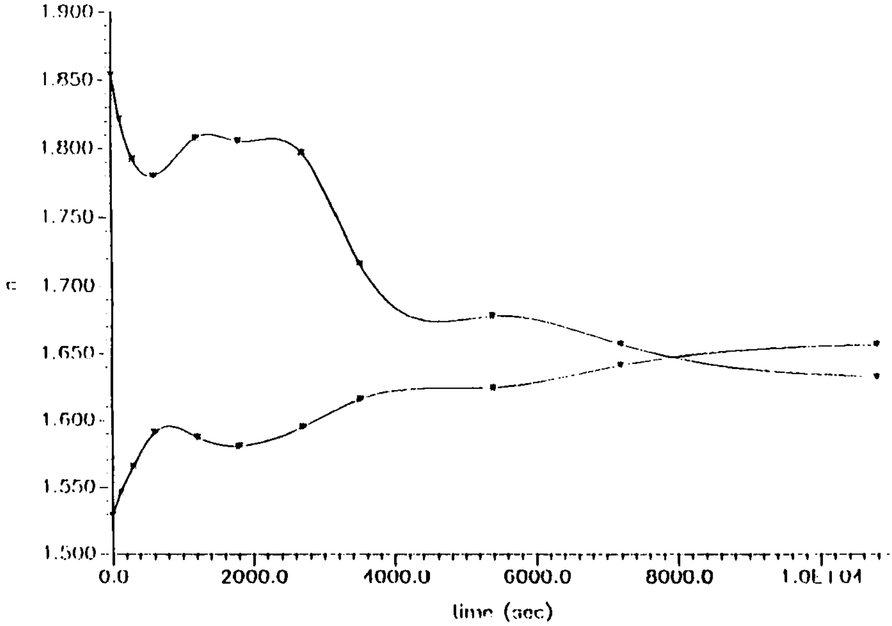

FIGURE 9 Variation of the refractive indices of the monodomain as a function of the irradiation time using polarized light.

of the molecules undergoing an isomerization cycle as far as their original orientation is concerned.

3. The active azobenzene molecules are held in the glassy matrix. As a result there is no Brownian motion or any other effect which drives the molecules back to their original orientation distribution after having changed their orientation under the influence of an isomerization process.

4. The molecules are continuously subjected to the isomerization cycle during irradiation and the corresponding reorientational motions unless the transition dipole moment is perpendicular to the polarization direction of the light. The final state of orientation is one in which all chromophores fulfill this requirement.

The derivation of the relevant rate equations start from those characteristic for photostationary systems in the melt or in solution.

$$\frac{d[A]}{dt} = \frac{I_{\mathrm{abs}}^{\mathrm{tot}}}{E}\, d[\varphi_{BA}\varepsilon_B[B] - \varphi_{AB}\varepsilon_A[A]]$$

$$\frac{d[B]}{dt} = \frac{I_{\mathrm{abs}}^{\mathrm{tot}}}{E_{\mathrm{tot}}}\, d[\varphi_{AB}\varepsilon_A[A] - \varphi_{BA}\varepsilon_B[B]]$$

$[A]$, $[B]$ is the concentration of the species A and B; ε_A, ε_B are the molar extinction coefficients; φ_{AB}, φ_{BA} are the respective quantum yields; and E_{tot} is the total extinction for a cell with a thickness of d.

Under certain assumptions (see above) these equations can be extended to the solid state.

1. In the solid state the concentration has to be replaced by the orientation distribution functions $f_A(\Omega)$ and $f_B(\Omega)$ which represent the concentration of molecules for every distinct solid angle.

2. The molecular extinction is replaced by the square of the product of the transition dipole moment and the vector of polarization.

3. The rotational diffusion step is represented by a transfer function $F_{AB}(\Omega\ \Omega')$ which gives the probability for a molecule pointing into Ω after a reaction provided its initial orientation was given by Ω'.

The total change of the orientation distribution function is then given by the integral over all Ω' which turn into Ω, multiplied with the rate of reacting molecules. The result is as follows:

$$\frac{d}{dt} f_A(\Omega) = \frac{I_{\text{abs}}^{\text{tot}}}{E_{\text{tot}}}\, d \left[\varphi_{BA} \int_{\Omega'} F_{BA}(\Omega', \Omega) f_B(\Omega')(\mathbf{M}_B(\Omega')\mathbf{e}_\varphi)^2\, d\Omega' \right.$$

$$\left. - \varphi_{AB}(\mathbf{M}_A(\Omega)\mathbf{e}_\varphi)^2 f_A(\Omega) \right]$$

$$\frac{d}{dt} f_B(\Omega) = \frac{I_{\text{abs}}^{\text{tot}}}{E_{\text{tot}}}\, d \left[\varphi_{AB} \int_{\Omega'} F_{AB}(\Omega', \Omega) f_A(\Omega')(\mathbf{M}_A(\Omega')\mathbf{e}_\varphi)^2\, d\Omega' \right.$$

$$\left. - \varphi_{BA}(\mathbf{M}_B(\Omega)\mathbf{e}_\varphi)^2 f_B(\Omega) \right]$$

It is first of all apparent that one stationary solution exists which corresponds to an orientation distribution function where all molecules are perpendicular to the initial vector of polarization, as experimentally observed (see Figure 8).

In addition dynamic solution can be obtained. In order to make predictions one has to select an appropriate transfer function. We selected one with a Gaussian shape

$$F_{AB}(\Delta\xi) = Ae^{-n\sin^2(\Delta\xi)}$$

The width of the distribution which is controlled by the parameter n represents in this case something like the rigidity of the matrix. A rigid matrix (n = inf) reorients the dye molecules always back to the original distribution whereas a completely soft matrix does not give rise to any effective restoring force ($n = 0$). The comparison of such predictions with experimental results shows that the predictions of the rate equation based on this rather crude concept agree quite well with the experimental results. An example in case is shown in Figures 10 and 11 which represent the time development of the reorientation of the optical axis as

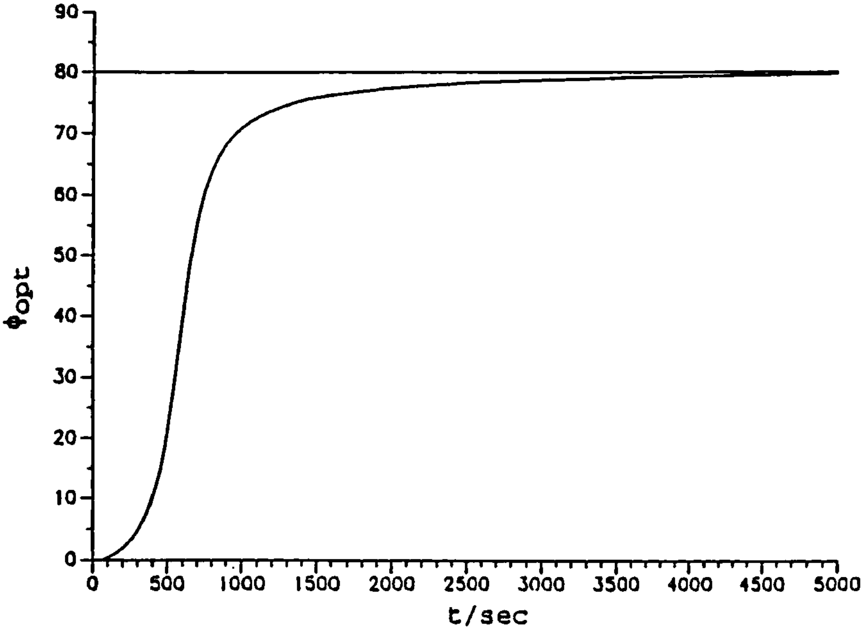

FIGURE 10 Theoretically predicted time evolution of the reorientation angle.

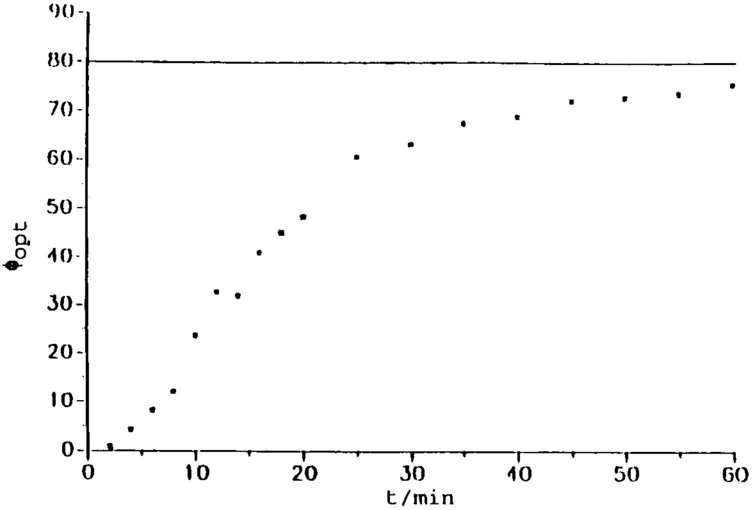

FIGURE 11 Experimentally determined time evolution of the reorientation angle.

observed experimentally. It thus seems that side chain liquid crystalline polymers can be characterized as rather soft matrices.

Two other aspects will briefly be mentioned. First of all the expectation is that the reorientation angle should not so much depend on the intensity I of the light but rather on the total energy E supplied to the system ($E = I \cdot t$). Figure 12 shows results consistent with this expectation.

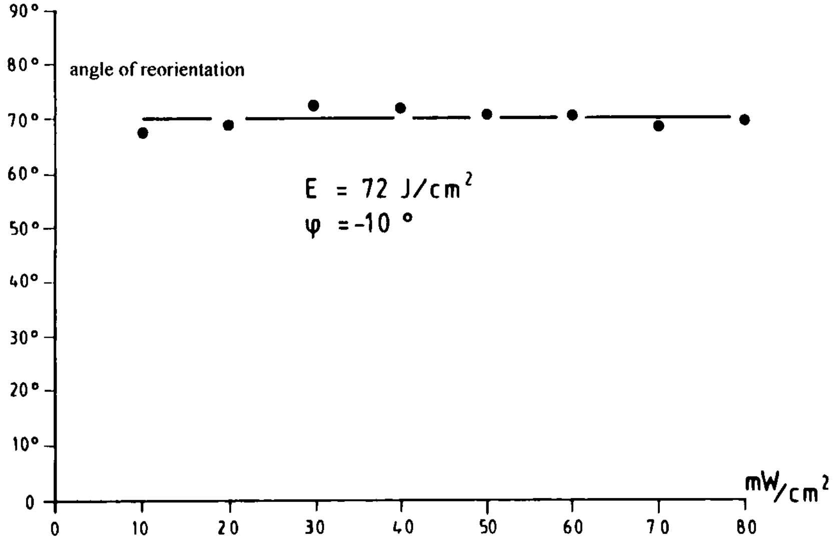

FIGURE 12 Dependence of the reorientation angle on the intensity of the light.

Another very interesting consequence of the model introduced in this chapter is that the resolution should in principle be controlled by the size of a chromophore as apparent from the assumption 1 of the model: only those groups can change their orientation which undergo such an isomerization cycle. We have called this effect molecular addressing.[23]

V. GRATING EXPERIMENTS

In order to test the capability of the liquid crystalline polymers with respect to the storage of holograms we performed grating experiments.[24] A stable and vibration-damped optical table has to be used for such interference experiments (Figure 13). Gratings are conveniently obtained by using a two beam interference of plane waves in a Mach Zehnder interferometer. An argon ion laser operating at 488 nm single mode single frequency was used by us as the light source. Spatial frequencies between 10 and 3000 lines/mm were achieved by varying the angle of the intersection according to:

$$\Delta = \lambda/2 \sin(\theta/2)$$

where Δ: fringe spacing.

Tubes were placed in the arms of the interferometer to avoid disturbances due to air convection, the irradiation time could be extended up to nearly 3 hours. The diffraction efficiency which is one of the relevant parameters to be characterized is given by

$$\eta_m = I_m/I^0$$

for the *m*th order of refraction.

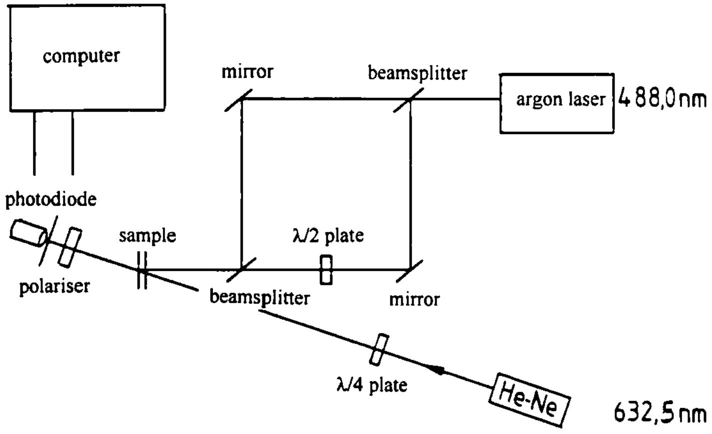

FIGURE 13 Experimental set up used for the grating experiments.

It is helpful to be able to probe the induced optical modulation during the recording process. The set-up allowing this is shown in Figure 13. We used a helium neon laser operating at 632.8 nm for the probing. The diffracted intensities were recorded by a photodiode.

Later on we will discuss polarization holography where the polarizations of the object beam and the reference beam are not parallel. In this case a λ/2 plate is placed in one arm of the interferometer to turn the direction of polarization. The grating is then detected by circular polarized light of a He-Ne laser operating at 632.8 nm. To measure the intensity in the first diffractive order as a function of time and polarization a polarizer and a photodiode were used. The resulting signal was divided by the value of the detecting laser beam at the same polarization but measured before the irradiation process.

Typical results for the growth of the induced grating (parallel polarization of object and reference beam) and the diffraction efficiencies observed are shown in Figures 14 and 15. Figure 14 displays the growth of the induced modulations for various writing intensities and Figure 15 shows, for example, the first order diffraction efficiency as a function of the spatial frequency as measured for the liquid crystalline monodomain films. As this diagram shows small structures can be recorded very effectively. The very high diffraction efficiency which can be achieved combined with an excellent resolving power makes this type of liquid crystalline polymer an attractive novel recording medium.

Actually we were able to store real holograms reversibly in such materials and we were also able to prepare holographic optical components, such as a Fresnel lens, using azobenzene containing liquid crystalline side chain polymers. This has been documented in the literature. Yet one specific feature of the material which makes it different from the conventional holographic storage materials has not been taken into account so far: it stores in principle not only information on the intensity but also on the state of polarization of the light. It can thus be used for polarization holography.

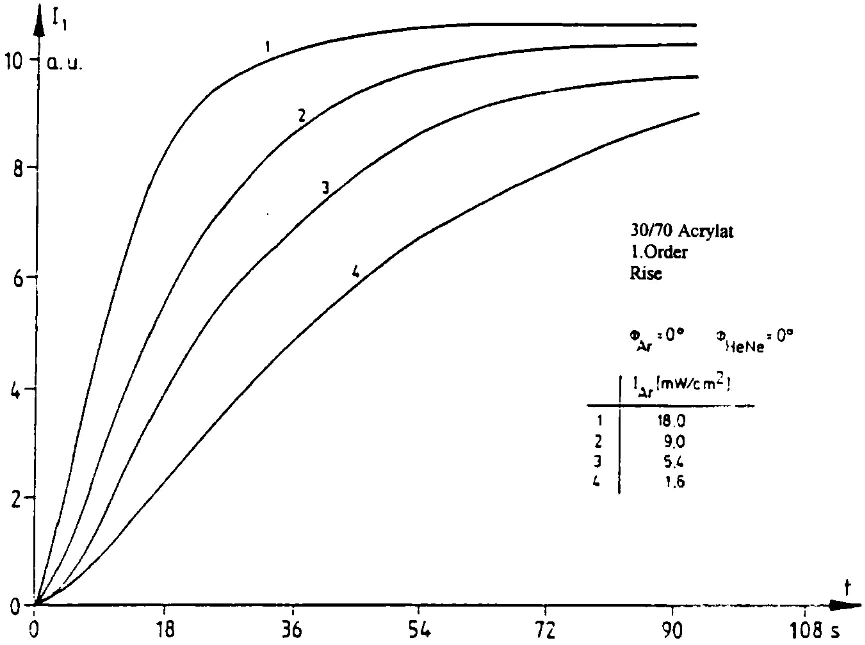

FIGURE 14 Growth of the induced modulations (grating experiment) for various writing intensities.

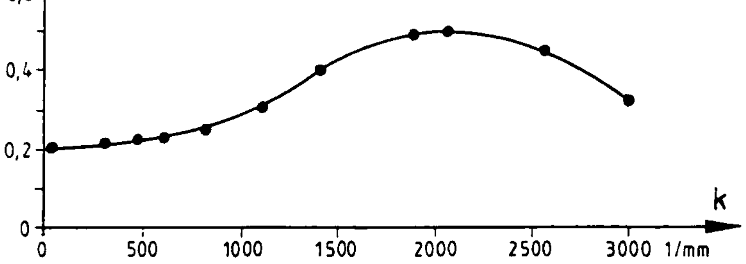

FIGURE 15 First order diffraction efficiency as a function of the spatial frequency.

VI. POLARIZATION HOLOGRAPHY[15,16,25–27]

It has been pointed out above that the characteristic feature of holographic recording is the transformation of phase information into intensity using the interference of the beam carrying the information (object beam) with a reference beam. The reason is that optical storage media are not able to record phase information directly. Optical recording media have still another disadvantage. The pattern recorded does not contain information on the state of polarization of the incident light. So if the surface of the object to be recorded has the property of changing the polarization of the reflected light one will not be able to store this information in the hologram. Sometimes this kind of information may be crucial. Polarization holography is the answer.

It has become apparent above that the material described here is to a certain extent able to store information on the polarization of the light: it tends to change the direction of its main optical axis which approaches a saturation value of 90° relative to the polarization direction. So in principle this material may be capable of storing polarization holograms. To test this capability it is again favorable to perform grating experiments. The following part will be concerned with a discussion of how to obtain gratings based on the superposition of beams with different polarization, how such gratings are stored in the liquid crystalline materials and finally we will discuss the read out.

So at first we consider the superposition of two beams with different polarization and intensity the propagation vector k of which is characterized by an angle $\delta/2$ with respect to the x-axis (Figure 16). We obtain for the y-direction:

$$\mathbf{E}_1 = E_0\mathbf{e}_z e^{i(-|k|y\sin(\delta/2)-\omega t)}$$

$$\mathbf{E}_2 = E_0[\mathbf{e}_z \cos\varphi + \mathbf{e}_y \sin\varphi \cos(\delta/2) + \mathbf{e}_x \sin\varphi \sin(\delta/2)]e^{i(|k|y\sin(\delta/2)-\omega t)}$$

The first wave is thus polarized along the z-direction and the polarization of the second wave is tilted by the angle φ with respect to the z-axis. $|k|$ is defined as $|k| = 2\pi/\lambda$. We will limit our discussion to the two cases: $\varphi = 0°$ (parallel polarization) and $\varphi = 90°$ (perpendicular polarization).

The superposition of the two waves results in the following intensity distribution in the first case (parallel polarization)

$$I = 4E_0^2\left[1 + \cos\left(2\pi\frac{2}{\lambda}y\sin(\delta/2)\right)\right]$$

This is a cos-grating with a spatial frequency of $\Delta = \lambda/(2\sin(\delta/2))$.

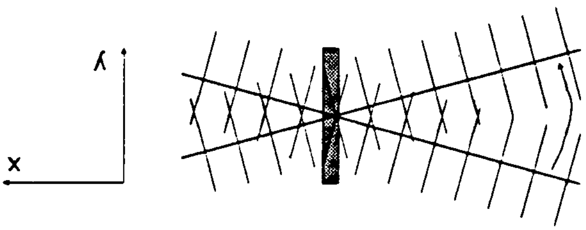

FIGURE 16 Superposition of two beams with different directions of polarization.

FIGURE 17 Polarization grating as predicted by theory.

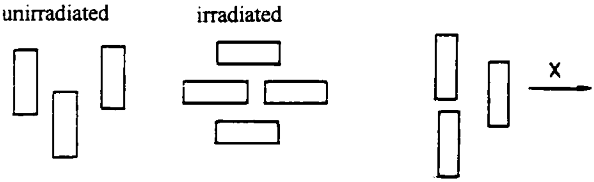

FIGURE 18 Schematic diagram for the distribution of molecular axes in a simple polarization grating.

In the case of perpendicular polarized waves the electric field vector turns out to be

$$\mathbf{E} = E_0[\mathbf{e}_z e^{-i\Phi} + \mathbf{e}_x \sin(\delta/2)e^{i\Phi} + \mathbf{e}_y \cos(\delta/2)e^{i\Phi}]e^{-i\omega t}$$

with

$$\Phi = \frac{2\pi}{\lambda}\, y \sin(\delta/2)$$

The intensities ($I = EE^*$) are thus independent of the phase Φ. So a polarization grating periodic in π is obtained, in contrast to an amplitude grating periodic in π obtained for $\varphi = 0$. The relation given above will be discussed for different phases Φ. Due to the fact, that δ is taken to be small, the component in the x-direction can be neglected.

1. $\Phi = 0$ $\quad \mathbf{E} = E_0[\mathbf{e}_z + \mathbf{e}_y]e^{-i\omega t}$
2. $\Phi = \pi/4$ $\quad \mathbf{E} = E_0/\sqrt{2}[(\mathbf{e}_y + \mathbf{e}_z) + i(\mathbf{e}_y - \mathbf{e}_z)]e^{-i\omega t}$
3. $\Phi = \pi/2$ $\quad \mathbf{E} = E_0[i(\mathbf{e}_y - \mathbf{e}_z)]e^{-i\omega t}$
4. $\Phi = 3/4\pi$ $\quad \mathbf{E} = E_0/\sqrt{2}[-(\mathbf{e}_y + \mathbf{e}_z) + i(\mathbf{e}_y - \mathbf{e}_z)]e^{-i\omega t}$

So the state of polarization varies periodically as a function of ϕ and thus of y as shown schematically in Figure 17. Cases 1. and 3. describe linearly polarized light, with the polarizations tilted ±45° with respect to the z-axis. The expressions for the cases 2. and 4. describe right and left circularly polarized light. The grating is a mixture of amplitude and polarization gratings for $0° < \varphi < 90°$.

Next we will consider the effect of such a polarization grating on the storage material considered here considering at first parallel polarization directions of object and reference beam. The irradiation with an s-polarized grating leads to a relative simple structure as shown in Figure 18. No change of orientation will take place within the unirradiated areas and the molecular groups are reoriented by 90° in the irradiated areas. The refractive indices in this area will change consequently.

The principal optical axis will still be oriented along the direction of the polarization of incident light. Thus the refractive indices (n_z and n_y) will change periodically, without any change of the principal axis. This can be described by

$$n_y(y) = \frac{n_y^b + n_y^u}{2} + \frac{1}{2}(n_y^b - n_y^u)\sin(y/\Lambda) = \tilde{n}_y + \frac{1}{2}\Delta n_y \sin(y/\Lambda)$$

where n_y is the ordinary refractive index.

Next we will consider the read out (diffraction) of the stored grating using circular polarized light. The analysis predicts that the intensity displays diffractive maxima of order q at

$$y = \frac{q\lambda}{2\pi\Lambda}x$$

with diffraction efficiencies of:

$$\eta_q = I_q/I_0 = J_q^2(f\Delta n_i/2)$$

Thus both beams (y- and z-polarized) are predicted to be diffracted to the same places but with different intensities. The phase difference between the two beams (due to the average refractive index) is

$$\Delta = f(\tilde{n}_z - \tilde{n}_y)$$

with

$$f = 2\pi d/\lambda$$

For $\Delta = \pi/2$ the incident circular polarized light will lead to elliptically polarized light with different directions of the principal axis in different orders q of the diffraction. A very interesting case is the one where $\Delta n_y = 0$. The light is linearly z-polarized in all orders q which is very interesting for polarization holography. The problem is to realize a reference wave such that $\Delta n_{i+90°} = 0$ (where i is the given polarization of the object wave).

The discussion on the optical pattern induced in the storage material by the polarization grating (using different polarization directions) as well as on the read out behavior using circularly polarized light will be quite complex, it goes well beyond the scheme of this contribution. It is sufficient to point out that an optically biaxial structure is induced in those locations which are illuminated (one axis along z the other along x) and that the interaction of circularly polarized light with such an optical pattern will have strong effects on quantities such as the angular distribution of the maximum diffraction efficiency, the ratio of the polarization of the incident and the diffracted beam, etc.

Next we will introduce experimental results. At first some results obtained for a parallel polarization of the two beams will be considered. The quantities of interest

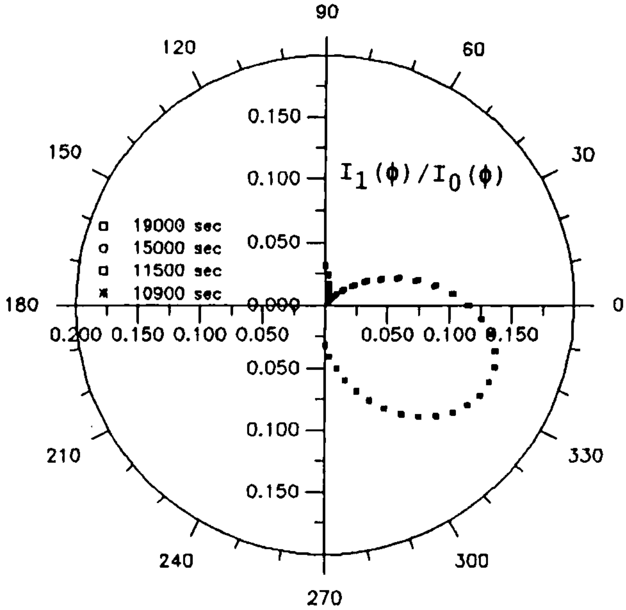

FIGURE 19 Illustration of the diffraction efficiency as a function of the irradiation time (polar diagram).

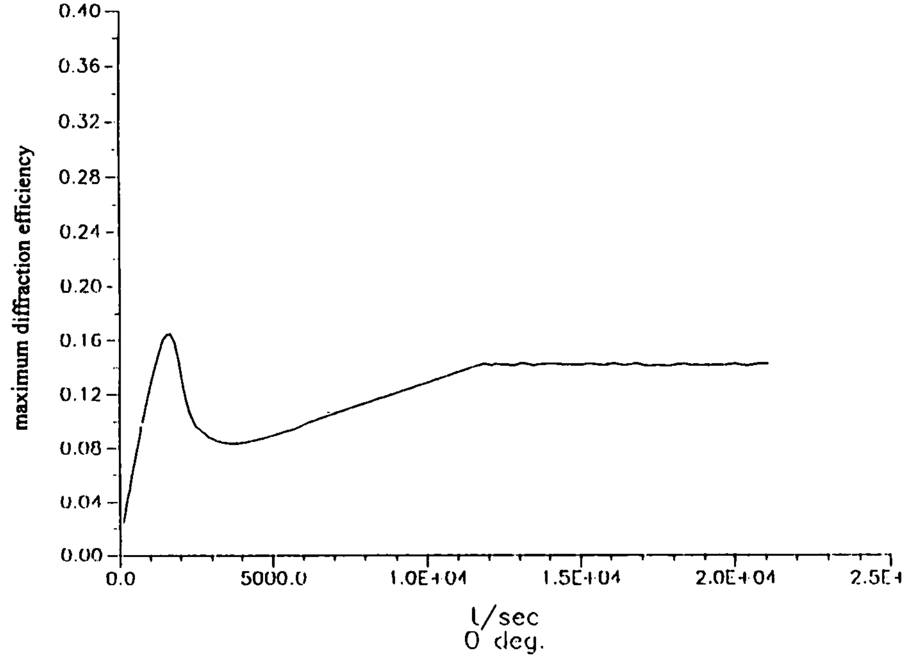

FIGURE 20 Maximum diffraction efficiency as a function of the irradiation time, parallel polarizations of intersecting beams.

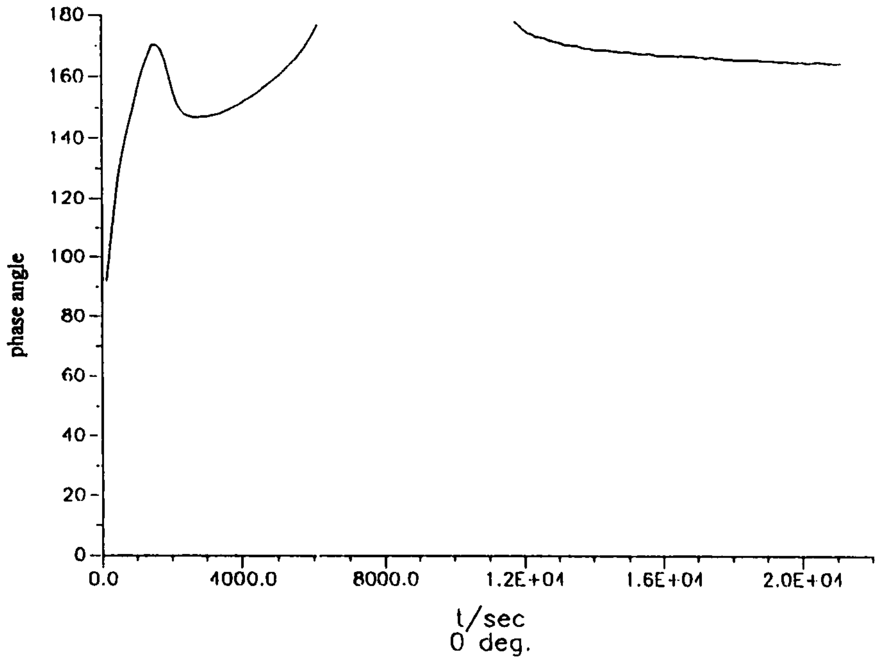

FIGURE 21 Phase angle as a function of the irradiation time, parallel polarizations of intersecting beams.

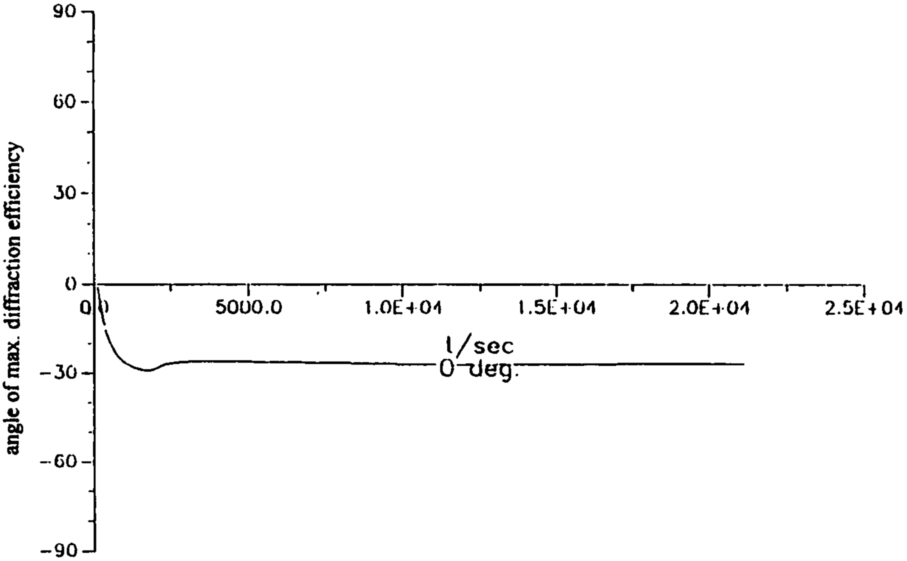

FIGURE 22 Angle of maximum diffraction efficiency as a function of the irradiation time, parallel polarizations of intersecting beams.

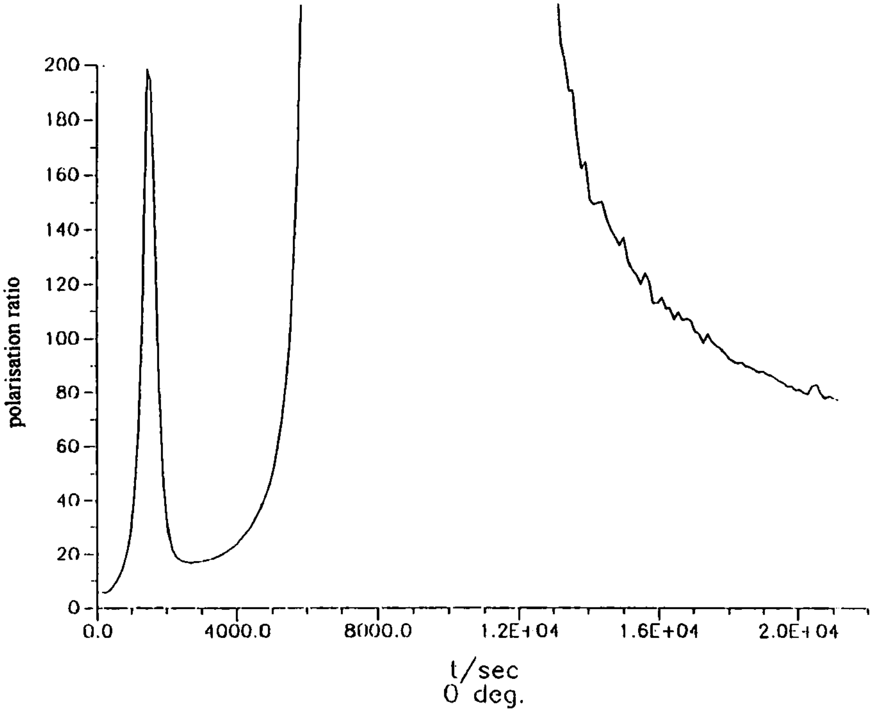

FIGURE 23 Polarization ratio as a function of the irradiation time, parallel polarizations of intersecting beams.

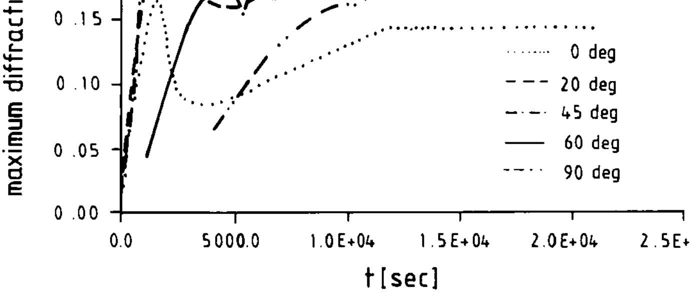

FIGURE 24 Maximum diffraction efficiency as a function of the irradiation time, nonparallel polarizations of intersecting beams.

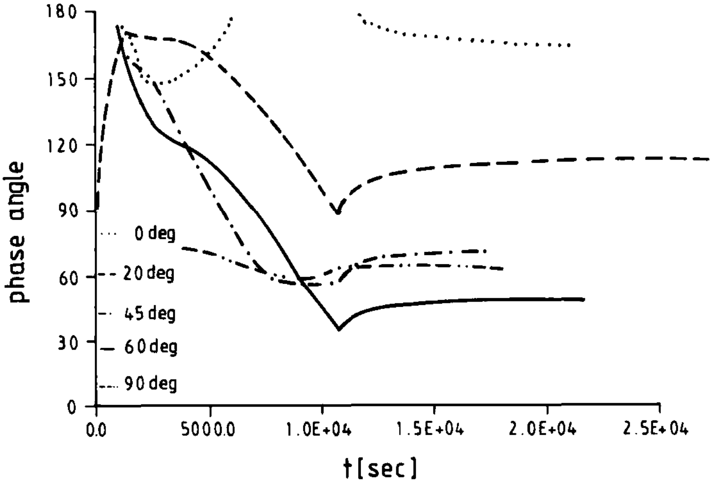

FIGURE 25 Phase angle as a function of the irradiation time, nonparallel polarizations of intersecting beams.

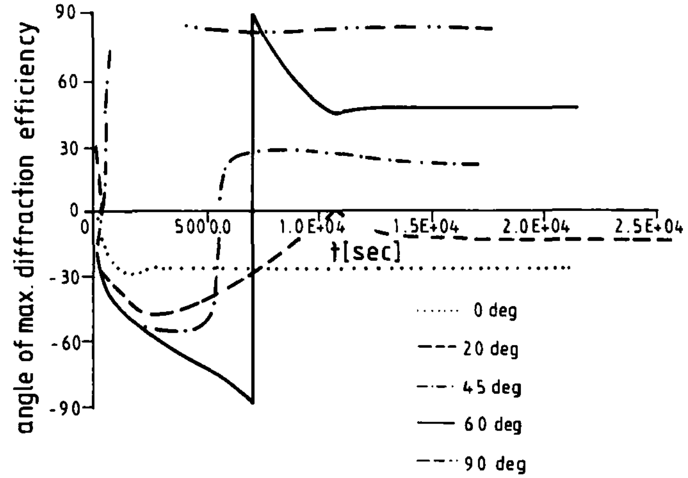

FIGURE 26 Angle of maximum diffraction efficiency as a function of the irradiation time, nonparallel polarizations of intersecting beams.

are the polar angle for which the maximum diffraction efficiency is observed (relative to the z-direction), the maximum diffraction efficiency itself, the polarization ratios (ratio of the maximum to the minimum diffraction efficiency, which is a measure of the degree of linear polarization of the diffracted beam) and finally the phase angle between the z- and y-polarized partial beams. The first three quantities are especially interesting for judging the capabilities of the material for polarization holography. The phase difference is useful for the comparison of the results obtained from UV-dichroitic with those obtained from grating index experiments.

Figure 19 shows as an illustration the development of the diffraction efficiency as a function of time in a polar diagram. It is apparent that the angle of maximum diffraction efficiency is about 30° and is independent of the irradiation time. Next we will consider the quantities mentioned above in more detail.

Maximum Diffraction Efficiency (Figure 20)

The diffraction efficiencies increase with time for shorter irradiation times. Remarkable is the first maximum of the diffractive efficiency. Its occurrence is probably the consequence of the onset of the isomerization cycles. A constant value of about 0.16 is obtained for longer irradiation times. The gap apparent for intermediate irradiation times is due to interpolation problems, this problem occurred also for the analysis of the data presented in the following figures.

Phase Angle (Figure 21)

The phase angle describes the phase difference between z- and y-polarized beam. Due to the circular polarization this angle is 90° in front of the grating. Again a maximum is observed for shorter times as in the case of the diffractive efficiency. The light which has been diffracted by the grating is nearly linearly polarized as apparent from the data on the phase angle and polarization ratio.

Angle of Maximum Diffractive Efficiency (Figure 22)

The angle of maximum diffraction efficiency increases with increasing irradiation time for short times and saturates at an angle of 30° (see polar diagram).

Polarization Ratio (Figure 23)

The polarization ratio approaches very high values for longer irradiation times after having displayed a local maximum for shorter irradiation times. This is consistent with the results discussed above for the phase angle.

So it is obvious that the material is able to store to a certain extent information related to polarization and that one is able to retrieve such information using an unpolarized beam. The patterns obtained are, however, quite complex already for this special case. We are currently performing experiments to try to develop an understanding of the basic features in relation to the processes happening during storage in the liquid crystalline polymers.

In the following we will analyze the even more complex case that the angle between the two polarization directions is varying between 0 and 90°. This angle is the parameter in all diagrams to follow.

In the case of the maximum diffractive efficiency (Figure 24) the first maximum apparent in the diagram for 0° is shifted to longer irradiation times with increasing angle between the two beams. It is also apparent, that the diffraction efficiency assumes the lowest value for a parallel polarization and displays a maximum with more than one third of the maximum theoretical value for 20°. Taking this result and the one obtained for the polarization ratio it is apparent that the integral diffraction efficiency amounts to nearly 39% which is the maximum theoretical value. This is very surprising, because the grating is not a sin-grating after such long irradiation times.

The phase angles (Figure 25) definitely depend quite strongly on the angle of intersection of the polarization directions although is very difficult to draw a final conclusion since the phase angle did not approach a stationary state at the end of the experimental irradiation time. The phase angle decreases with increasing intersection angle, it only displays a maximum at intermediate irradiation times for an angle of 0°.

Another interesting result is the very characteristic dependence of the angle of maximum diffraction efficiency on the angle between the two writing beams as observed for long irradiation times (Figure 26). This dependence is important for the characterization of the material with respect to its capability to act as a storage material for polarization holography: the angle of maximum diffractive efficiency should be correlated with the polarization of the two writing beams. Although the curves show a correlation between these angles the deviation between the angle of the two incident beams and the angle of maximum diffractive efficiency is relatively large. The angles are nearly the same only in the case of 90°. This was proved also by experiments with other samples.

The polarization ratios as obtained for long irradiation times turned out to be very low especially at those points where the diffractive efficiency is large. It is still too early to arrive at a final judgment on the capability of the liquid crystalline material to be successive in the area of polarization holography. In any case the properties introduced above show that the potential is promising but also that the development of a more detailed understanding on the dynamic processes (isomerization) and the resulting optical properties (modification of birefringence, optical axes orientation) is a fundamental requirement for a future in such applications. In addition it should be mentioned that the concept discussed here can also be used for transient holography where the holographically stored information relaxes within a time scale of ms to s, depending on the application and where continuously new information is written in, using for instance a computer in connection with a laser scanner. Holographic and thus 3-dimensional displays are possible applications. We have performed corresponding experiments using azobenzene containing monomers.

Acknowledgment

We gratefully acknowledge the financial support of the Bundesministerium für Forschung und Technologie (BMFT)

References

1. M. Hartmann, B. J. A. Jakobs and J. J. M. Braat, *Philips Techn. Rev.*, **42**, 37 (1985).
2. D. J. Gravesteijn, C. J. van der Poel, L. O. Scholte and C. M. J. van Uitjen, *Philips. Techn. Rev.*, **44**, 250 (1987).
3. O. S. Heavens and R. W. Ditchburn, Insights into Optics, J. Wiley, New York (1987).
4. E. Hecht, Optics, Addison Wesley, Reading (1987).
5. H. Finkelmann, H. Ringsdorf and J. H. Wendorff, *Makromol. Chem.*, **179**, 273 (1978).
6. A. Ciferri (ed.), Liquid Crystallinity in Polymers, VCH Publishers, New York (1991).
7. A. Blumstein, Polymer Liquid Crystals, Plenum Press, New York (1985).

8. W. H. de Jeu, Physical Properties of Liquid Crystalline Material, Gordon and Breach (1979).
9. P. G. de Gennes, The Physics of Liquid Crystals, Clarendon Press (1974).
10. H. G. O. Becker Hrsg., Einführung in die Photochemie, Georg Thieme Verlag (1983).
11. H. Rau, *Angew. Chem.*, **85**, 248 (1973).
12. C. D. Eisenbach, *Makromol. Chem.*, **179**, 2489 (1978).
13. C. D. Eisenbach, *Makromol. Chem.*, **180**, 565 (1979).
14. M. Eich, PhD-thesis, TH Darmstadt (1987).
15. R. Birenheide, PhD-thesis, TH Darmstadt (1991).
16. K. Anderle, Master Thesis, TH Darmstadt (1991).
17. U. Wiessner, N. Reynolds, Ch. Boeffel and H. W. Spieß, *Makromol. Chem. Rapid Commun.*, **12**, 457 (1991).
18. S. Ivanov, I. Yakovlev, S. Kostromin and V. Shibaev, *Makromol. Chem. Rapid Commun.*, **12**, 709 (1991).
19. J. Stumpe, L. Müller, D. Kreysig, G. Hauck, H. D. Koswig, R. Ruhmann and J. Rübner, *Makromol. Chem. Rapid Commun.*, **12**, 81 (1991).
20. M. Eich and J. H. Wendorff, *Makromol. Chem. Rapid Commun.*, 8,467 (1986).
21. P. Hariharan, Optical Holography, Cambridge University Press, New York (1984).
22. R. Birenheide and J. H. Wendorff, *SPIE*, 1213 (1990).
23. K. Anderle, R. Birenheide and J. H. Wendorff, *Liq. Cryst.*, **5**, 691 (1991).
24. M. Eich and J. H. Wendorff, *J. Opt. Soc. of America B*, **7**, 1428 (1990).
25. R. V. Johnson and A. R. Tanguay, *Opt. Eng.*, **25**, 235 (1986).
26. O. V. Stolbova, *Sov. Phys. Dokl.*, **8**, 275 (1963).
27. T. Todorov, L. Nikolova and N. Tomova, *Appl. Optics*, **23**.